

APPLICATION OF A HIGH ACCURACY FINITE DIFFERENCE TECHNIQUE TO STEADY, FREE SURFACE FLOW PROBLEMS

RAYMOND S. CHAPMAN* AND CHIN Y. KUO†

Department of Civil Engineering, Virginia Polytechnic Institute and State University, Blacksburg, Virginia 24061, U.S.A.

SUMMARY

The spatially third-order accurate QUICK finite difference technique is applied to the solution of the depth-integrated equations of motion for steady, subcritical, free surface flow in a wide, shallow, rectangular channel with and without an abrupt expansion. The conservative, control-volume discretization of the equations of motion and the use of QUICK in approximating required cell and cell face average quantities is discussed. Results presented show that it is possible to obtain stable solutions for advective free surface flows without resorting to implicit numerical smoothing.

KEY WORDS QUICK Finite Difference Free Surface Flow

INTRODUCTION

With the growing interest in applying two-equation ($k - \varepsilon$) turbulence closure in numerical transport models,^{1–7} it is unfortunate to note that the finite difference techniques commonly employed fail to yield quantitatively acceptable results when applied to the problem of strong convective transport.⁸ The failure of these techniques to produce accurate results can often be attributed to inherent behavioural errors, such as artificial diffusion associated with upwind differencing and the wiggles characteristic of central differencing.⁹ As a result, the use of these techniques in turbulent flow simulations is questionable, in that it often becomes difficult to distinguish between the physical effects due to turbulence closure and numerical errors.^{10–12}

Recently, higher order finite difference techniques have been successfully applied to transport problems in both one and two dimensions.^{8,12–15} One of the more notable techniques for steady flow problems is the third-order accurate QUICK (Quadratic Upstream Interpolation for Convection Kinematics) method described by Leonard.⁸ The QUICK finite difference technique which is based on a conservative, control-volume integral formulation possesses the desirable convective stability of upwind differencing, but does not suffer from significant numerical diffusion.

In this paper, the QUICK differencing technique is applied to the solution of the depth-integrated equations of motion for steady, free surface flow in a wide, shallow, rectangular channel with and without an abrupt expansion. The results presented here are a

* Research Associate. Presently Research Engineer, Oceanweather, Inc., Vicksburg, MS 39180, U.S.A.

† Associate Professor

first step toward a test application of the two-equation ($k - \epsilon$) turbulence closure model in solving the depth-integrated equations of motion for steady free surface flows with separation.

DEPTH-INTEGRATED EQUATIONS OF MOTION

Under the assumption of a homogeneous, incompressible, viscous flow characterized by a hydrostatic pressure distribution, with wind and Coriolis forces neglected, the depth-integrated equations of motion are written^{16,17}

$$\frac{\partial h}{\partial t} + \frac{\partial(V_i h)}{\partial X_i} = 0 \quad (1)$$

$$\frac{\partial(V_i h)}{\partial t} + \frac{\partial(V_i V_j h)}{\partial X_j} + g \frac{\partial(h^2/2)}{\partial X_i} + gh \frac{\partial z_b}{\partial X_i} + \tau_{bi} - \frac{\partial T_{ij}}{\partial X_j} = 0 \quad (2)$$

in which $i, j = 1, 2$ and repeated indices require summation; V_i = two dimensional depth-averaged velocity vector (u, v); h = water depth; t = time, X_i = co-ordinate directions (x, y); g = acceleration due to gravity; z_b = channel bottom elevation above an arbitrary datum; τ_{bi} = components of the bottom shear stress per unit mass; and T_{ij} = components of the depth-integrated effective stress tensor per unit mass.¹⁶ The bottom stress terms are parametrized in accordance with the quadratic shear stress law, namely

$$\tau_{bi} = c V_i q \quad (3)$$

where $q = (u^2 + v^2)^{1/2}$ is the magnitude of the depth-averaged resultant velocity vector; and c is a friction coefficient computed from either Manning's or Chezy's equations. The depth-integrated effective stress tensor per unit mass is written as

$$T_{ij} = \int_{z_b}^{h+z_b} \left[\nu \left(\frac{\partial V_i}{\partial X_j} + \frac{\partial V_j}{\partial X_i} \right) - \overline{V'_i V'_j} - (\hat{V}_i - V_i)(\hat{V}_j - V_j) \right] dz \quad (4)$$

in which ν = kinematic viscosity; V'_i = horizontal turbulent velocity fluctuations; \hat{V}_i = three dimensional time averaged velocity components; and z = vertical co-ordinate direction. The contributions to the effective stress tensor are the viscous stresses, the turbulent Reynolds stresses, and the momentum dispersion terms which arise from the non-uniformity of the velocity profiles in the vertical direction. In the present work, the effective stress terms are neglected to eliminate any possibility of introducing explicit numerical smoothing for purposes of stabilizing the solution.

TWO-DIMENSIONAL 'QUICK' METHOD

Finite difference equations are obtained by integrating each of the equations of motion over the appropriate control cell on a constant space-staggered, square computational grid (Figure 1) and in time. For example, using a first-order time integration the x -momentum equation becomes

$$\overline{uh}^{n+1} = \overline{uh}^n - \frac{\Delta T}{\Delta S} \left\{ (\overline{uuh})_R^n - (\overline{uuh})_L^n + (\overline{vuh})_T^n - (\overline{vuh})_B^n + \frac{g}{2} [(h)_R^2 - (h)_L^2] \right\} + \Delta T (g \overline{h} S_x - c \overline{uq})^n \quad (5)$$

in which ΔT = time step; ΔS = space step; S_x = cell average bottom slope in the x -direction;

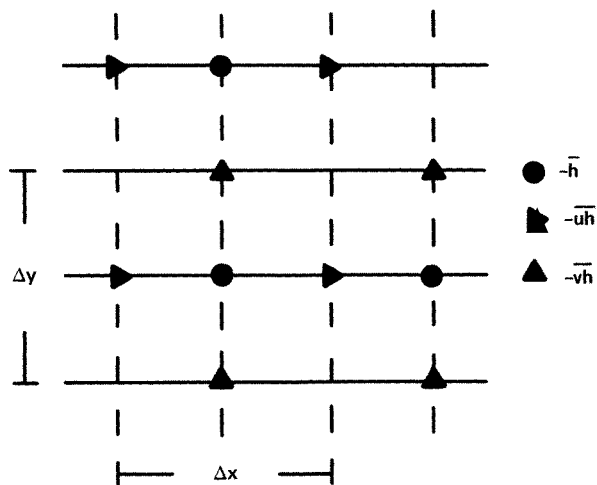


Figure 1. Computational grid

quantities in parentheses with subscripts R, L, T, B denote the right, left, top, and bottom cell face averages; and the overbar quantities denote cell averages (Figure 2). The required cell and cell face average quantities are approximated using a six-point upstream weighted quadratic interpolation surface.^{8,12} To illustrate the procedure, consider the computation of the right cell face average using the information provided in Figure 3. In this case, the u and v velocity components are both positive and directed to the right and up, respectively. Combining Newton's forward-difference formula in the longitudinal direction with Gauss's backward formula in the transverse direction, a quadratic interpolation function is constructed which reads¹⁸

$$f_{r,s} = (1 - r^2 - s^2 - sr)f_{0,0} + \left(\frac{r^2}{2} + \frac{r}{2} + sr\right)f_{1,0} + \frac{1}{2}(r^2 - r)f_{-1,0} + \frac{1}{2}(s^2 + s)f_{0,1} + \left(\frac{s^2}{2} - \frac{s}{2} + sr\right)f_{0,-1} - srf_{1,-1} \quad (6)$$

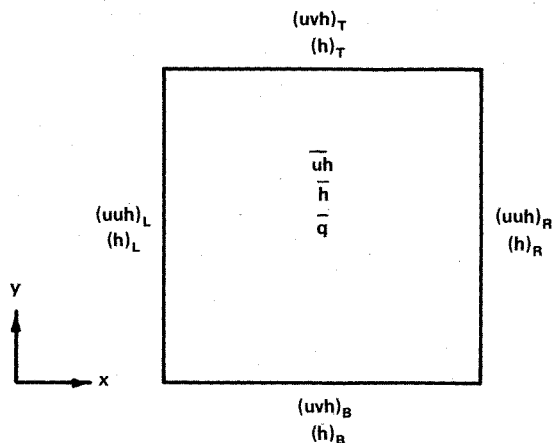


Figure 2. Computational cell for x-momentum equation

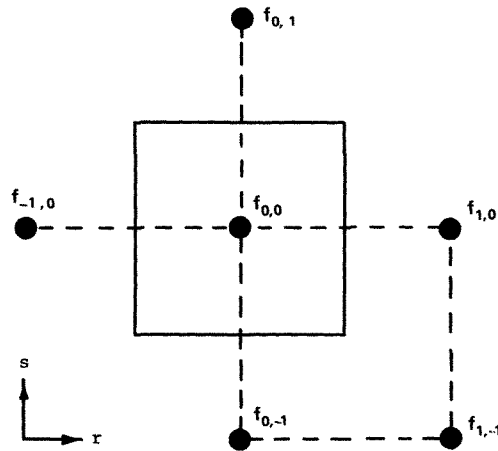


Figure 3. Required information for example cell face average computation

where $r = x/\Delta S$, and $s = y/\Delta S$ are local non-dimensional co-ordinates. The right cell face average is then computed as follows,

$$\begin{aligned}
 (f)_R &= \int_{-1/2}^{1/2} f_{1/2,s} ds \\
 &= \frac{1}{2} (f_{0,0} + f_{1,0}) - \frac{1}{8} (f_{1,0} - 2f_{0,0} + f_{-1,0}) \\
 &\quad + \frac{1}{24} (f_{0,1} - 2f_{0,0} + f_{0,-1})
 \end{aligned} \tag{7}$$

The spatial integration process used to obtain equation (5) is not strictly third-order in that as a means of reducing computational effort, it is necessary to assume that averages of products of field variables are reasonably estimated by products of the individual field variable averages. For example, computation of the right cell face average for the pressure term, requires that the depth along the cell face be redefined in terms of a cell face average and deviation, i.e.

$$h_R = (h)_R + h'_R \tag{8}$$

Then

$$\int_{-1/2}^{1/2} h_R h_R ds = (h)_R^2 + \int_{-1/2}^{1/2} h'_R h'_R ds \tag{9}$$

in which the integral on the right hand side is assumed small. In effect, this assumption restricts the difference in magnitudes of field variable deviations between opposing cell faces, and should be reflected in the allowable coarseness of the computational grid.

Finally, the appearance of the time derivative terms in the equations of motion should not be misinterpreted as an attempt to address unsteady flow phenomena. Strictly speaking, the QUICK method may only be applied to steady problems, and subsequently, the first-order time integration employed is simply a convenient way to iterate to a steady solution.

EXAMPLE PROBLEMS

The example problems chosen were flow in a wide rectangular channel with and without an abrupt expansion. The model inputs were a longitudinal bottom slope of 0.005, a transverse bottom slope of zero, a friction coefficient of 0.018, a grid spacing of 90 ft (27.45 m), and an upstream normal depth of 4.726 ft (1.441 m) which corresponds to an arbitrarily chosen flow rate per unit width of 30 ft³/s/ft (2.79 m³/s/m).

For the simple straight wall channel calculations, free-slip wall boundaries were employed which allowed a comparison of the computed water surface profile with a fourth order Runge-Kutta solution^{18,19} of the one-dimensional gradually varied flow equation.²⁰ The initial condition was to set all depths equal to the upstream normal depth, and all velocities equal to zero. At the downstream boundary, the depth was arbitrarily specified at 4.0 ft (1.22 m) and the velocity was computed by continuity. The upstream boundary condition was that of normal flow. Using a time step of 0.75 s, 540 iterations were required to satisfy a maximum difference of 0.01 per cent between the QUICK and Runge-Kutta solutions (Figure 4). The total number of grid points in the longitudinal direction was 100 of which half were depth, and half were velocity points. An average one-dimensional Courant number [$= \{q + \sqrt{gh}\} \Delta T / \Delta S$] for the steady solution was approximately 0.15.

The second example problem included an abrupt expansion with inlet and outlet channel widths of 360 ft (109.73 m) and 540 ft (164.59 m), respectively. At wall boundaries, both velocity components and the normal gradient in the water surface elevation were set to zero. This was accomplished by prescribing the value of image points outside the computational domain such that the interpolated cell face averages or gradients coincident with the wall were exactly zero. Symmetry was imposed at the channel centre line by requiring that the transverse gradients of the longitudinal velocity component and the depth were equal to zero. The transverse velocity component was treated as if the channel centre line was a wall boundary. The upstream and downstream boundaries were positioned sufficiently far from the expansion so that specification of uniform flow was appropriate. At the outset of the

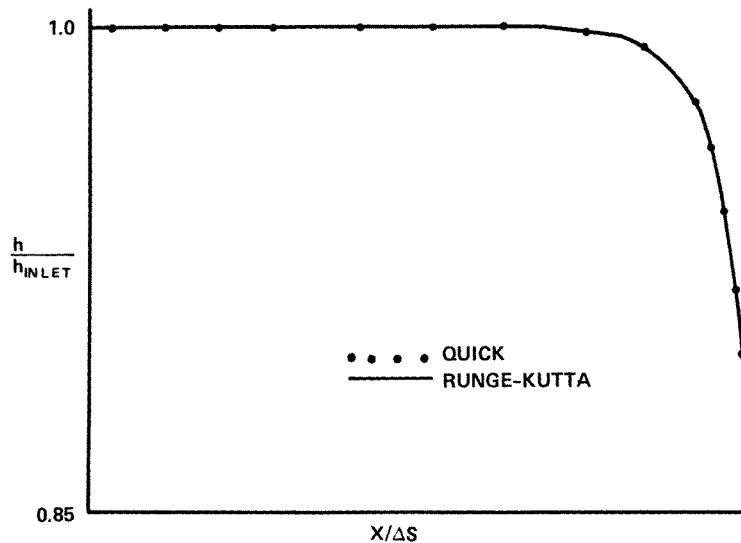


Figure 4. Comparison of computed water surface profiles for straight channel

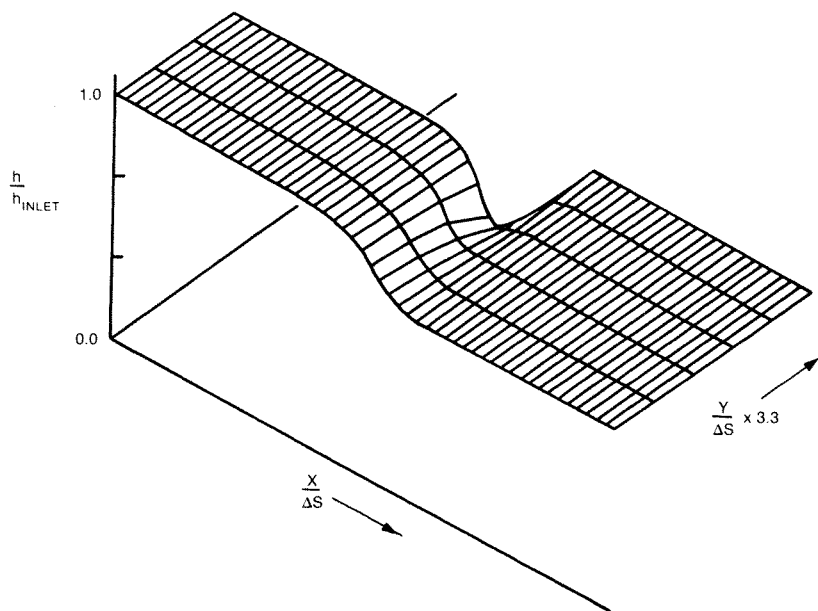


Figure 5. Computed water surface elevations for channel expansion

simulation, all depths were set equal to the upstream normal depth, and both velocity components were set to zero. In this calculation, 3500 iterations using a time step of 0.4 s yielded a solution which satisfied an error tolerance based on the difference between computed inflows and outflows of 0.01 per cent. An average two-dimensional Courant number $[= \{q + \sqrt{2gh}\} \Delta T / \Delta S]$ was found to be about 0.1, and the CPU time required was approximately 12 min on an IBM 3032. The results of the abrupt expansion calculation are presented in Figure 5, a three-dimensional plot of the water surface elevations and Figure 6, a plot of the depth-averaged velocity vectors.

The significance of the results presented becomes apparent when one attempts to repeat the test computations using linear interpolation for cell and cell face averages, i.e. central differencing. In trial runs with both the one and two-dimensional problems, central differencing failed to produce steady solutions in either case. The inability of the forward time central space difference procedure to achieve stable, monotonic solutions results from the well-known static instability wiggles, which ultimately caused the computations to breakdown.

Interestingly enough, the disastrous effect of wiggles is independent of whether the advective transport terms are linear, as in the case of scalar transport with a uniform velocity

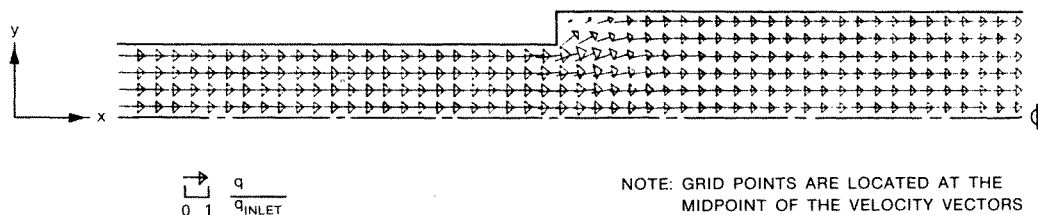


Figure 6. Computed depth-averaged velocity field for channel expansion

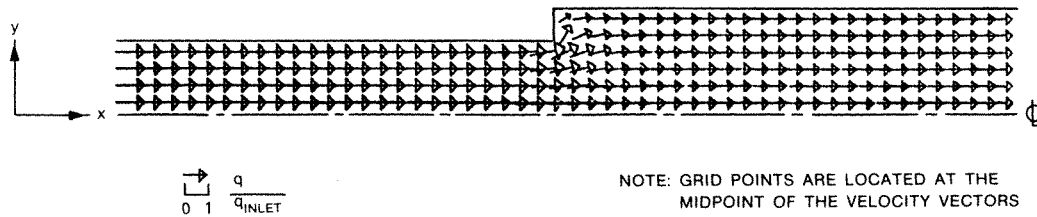


Figure 7. Computed depth-averaged velocity field for channel expansion with the non-linear advective acceleration terms omitted

field, or non-linear, as in the present study.⁹ The significance of retaining the non-linear advective acceleration terms was investigated by simply setting these terms to zero in the momentum equations, (equation (2)), and repeating the channel expansion simulation using both QUICK and the central difference procedure. As expected, QUICK provided a steady state solution quite similar to that depicted in Figure 6, however, with the exception of local differences seen in the velocity field in the corner region (Figure 7). The analogue of Figure 5, which exhibited no detectable differences at the scale plotted, is not presented. On the other hand, the central difference procedure again failed to converge to a steady solution. Although non-convergence is not surprising, it is interesting to note that the central difference calculation with the non-linear advective acceleration terms omitted required more than three times the number of iterations, prior to breaking down, than the simulation performed with the advective accelerations retained. This result clearly illustrates the aggravating effect of the non-linear advective acceleration terms and, consequently, suggests that the inherent advective stability exhibited by QUICK is an essential feature of any numerical technique that is to be applied in the modelling of complex free surface flows.

CONCLUSIONS

The spatially third-order accurate QUICK finite difference technique has been applied to the solution of the depth-integrated equations of motion for steady, free surface flow in a wide, shallow, rectangular channel with and without an abrupt expansion. Results presented show that it is possible to obtain stable, monotonic solutions to advective free surface flow problems without having to resort to implicit or explicit numerical smoothing. Comparison of the one-dimensional water surface profile computation with the Runge-Kutta calculation suggests that the QUICK technique is not only stable, but accurate.

Finally, based on the success with QUICK, to date, it is believed the computational procedure presented is an appropriate choice for a future test application of the two-equation ($k - \epsilon$) turbulence closure model in solving the depth-integrated equations of motion for steady, free surface flows with separation.

ACKNOWLEDGEMENT

The research is supported by the U.S. National Science Foundation (Grant Number CME-8004364).

REFERENCES

1. D. J. Atkins, S. J. Maskell and M. A. Patrick, 'Numerical prediction of separated flows', *Int. J. Num. Meth. Eng.* **15**, 129-144 (1980).
2. F. Durst and A. K. Rastogi, 'Theoretical and experimental investigations of turbulent flow with separation', *Proceedings, Symposium on Turbulent Shear Flows*, Penn. State Univ., Vol. 1, pp. 18.1-18.9, 1977.
3. A. D. Gosman, W. M. Pun, A. K. Runchal, D. B. Spalding and M. Wolfshtein, *Heat and Mass Transfer in Recirculating Flows*, Academic Press, London, 1969.
4. B. E. Launder and D. B. Spalding, 'The numerical calculation of turbulent flows', *Computer Methods in Applied Mechanics and Engineering*, **3**, 269-289 (1974).
5. M. A. Leschziner and W. Rodi, 'Calculation of strongly curved open channel flow', *Journal of the Hydraulic Division, ASCE*, **105**, (HY10), 1297-1314, October (1979).
6. J. J. McGuirk and W. Rodi, 'A depth-averaged mathematical model for the near field of side discharges into open channel flow', *Journal of Fluid Mechanics*, **86**, (4), 761-781 (1978).
7. A. Rastogi and W. Rodi, 'Prediction of heat and mass transfer in open channels', *Journal of the Hydraulic Division, ASCE*, **HY3**, 397-420 (1978).
8. B. P. Leonard, 'A stable and accurate convective modeling procedure based on quadratic upstream interpolation', *Computer Methods in Applied Mechanics and Engineering*, **19**, 59-98 (1979).
9. P. J. Roache, *Computational Fluid Dynamics*, Hermosa Publishers, Albuquerque, NM, 1972.
10. I. P. Castro, 'Numerical difficulties in the calculation of complex turbulent flows', *Proceedings, Symposium on Turbulent Shear Flow*, Penn. State Univ., Vol. 1, pp. 5.13-5.21, 1977.
11. G. H. Lean and T. J. Weare, 'Modeling two-dimensional circulating flows', *Journal of the Hydraulic Division, ASCE*, **105**, (HY1), 17-26 (1979).
12. B. P. Leonard, M. A. Leschziner, and J. McGuirk, 'Third-order finite-difference method for steady two-dimensional convection', *Proceedings of the International Conference on Numerical Methods in Laminar and Turbulent Flow*, Swansea, 807-819, July, 1978.
13. M. B. Abbott and C. H. Rasmussen, 'On the numerical modeling of rapid expansions and contractions in models that are two-dimensional in plan', *Paper A104, 17th IAHR Congress*, Baden-Baden, Germany, pp. 229-237, 1977.
14. P. Hinstrup, A. Kej and U. Kroszynski, 'A high accuracy two-dimensional transport-dispersion model for environmental applications', *Paper B17, 17th IAHR Congress*, Baden-Baden, Germany, pp. 129-137, 1977.
15. F. M. Holly and A. Preissman, 'Accurate calculation of transport in two dimensions', *Journal of the Hydraulic Division, ASCE*, **103**, (HY11), Proc. Paper 13336, pp. 1259-1277, November (1977).
16. C. Flokstra, 'The closure problem for depth averaged two-dimensional flows', 1 *Paper A106, 17th IAHR Congress*, Baden-Baden, Germany, pp. 247-256, 1977.
17. J. Kuipers and C. B. Vreugdenhil, 'Calculation of two-dimensional horizontal flow', *Report S 163-I*, Delft Hydraulics Laboratory, 1973.
18. F. B. Hildebrand, *Introduction to Numerical Analysis*, McGraw-Hill, New York, 1956.
19. F. M. White, *Viscous Fluid Flow*, McGraw Hill, New York, 1974.
20. V. T. Chow, *Open Channel Hydraulics*, McGraw-Hill, New York, 1959.